PLANT SCIENCE

Cell-cell adhesion in plant grafting is facilitated by β-1,4-glucanases

Michitaka Notaguchi[1,2,3,4]*, Ken-ichi Kurotani[1], Yoshikatsu Sato[3,5], Ryo Tabata[2], Yaichi Kawakatsu[2], Koji Okayasu[2], Yu Sawai[2,4], Ryo Okada[2], Masashi Asahina[6], Yasunori Ichihashi[7,8], Ken Shirasu[7,9], Takamasa Suzuki[10], Masaki Niwa[2,4], Tetsuya Higashiyama[3,5,9]

Plant grafting is conducted for fruit and vegetable propagation, whereby a piece of living tissue is attached to another through cell-cell adhesion. However, graft compatibility limits combinations to closely related species, and the mechanism is poorly understood. We found that *Nicotiana* is capable of graft adhesion with a diverse range of angiosperms. Comparative transcriptomic analyses on graft combinations indicated that a subclade of β-1,4-glucanases secreted into the extracellular region facilitates cell wall reconstruction near the graft interface. Grafting was promoted by overexpression of the β-1,4-glucanase. Using *Nicotiana* stem as an interscion, we produced tomato fruits on rootstocks from other plant families. These findings demonstrate that the process of cell-cell adhesion is a potential target to enhance plant grafting techniques.

Plant grafting has been applied to improve crop traits for thousands of years (*1*). Wound healing allows growth of two or more segments of connected plant tissue to grow as a single plant (*2*–*4*). Grafting has been used to propagate fruit trees and vegetables. With grafting, root (stock) characteristics, such as disease resistance and tolerance of unfavorable soil conditions, can support growth of favored fruit and vegetable characteristics from the shoot (scion) (*1*, *5*). Grafting is also used to study systemic signaling in plants and long-distance vascular transport (*6*–*9*). Although grafting is most successful between members of the same family (*2*–*4*, *6*), several interfamily graft combinations have been reported (*10*–*14*): A *Nicotiana benthamiana* scion (*Nb*, Solanaceae) can be grafted onto an *Arabidopsis thaliana* stock (*At*, Brassicaceae) (*15*), although the *Nb* scion grows slowly (fig. S1 and movie S1).

Here, we studied interfamily graft combinations. We observed that *Nicotiana* shows grafting potential with phylogenetically distant plant species: Interfamily grafts survived for more than 1 month (Fig. 1 and tables S1 and S2). With *Chrysanthemum morifolium* (*Cm*, Asteraceae), we conducted *Cm*/*Cm* homografts (scion/stock notation) and interfamily grafts with *Glycine max* (*Gm*, soybean, Fabaceae) and *Nb*. *Cm*/*Cm* homografts established and the *Cm* scions produced flowers, whereas the *Gm*/*Cm* interfamily grafts did not establish and the *Gm* scions died (Fig. 1, A and B). By contrast, in *Nb*/*Cm* interfamily grafts, the *Nb* scions established and grew (Fig. 1C). The *Nb* scion grew for more than 3 months until setting seeds. *Nicotiana* interfamily grafting was also successful with *Nb* as the stock (fig. S1C).

In transverse sections of the graft junctions, a necrotic layer was visible at the graft boundary in unsuccessful *Gm*/*Cm* interfamily grafts but developed only weakly in successful *Cm*/*Cm* homografts and *Nb*/*Cm* interfamily grafts 2 weeks after grafting (Fig. 1, D to F). Necrotic layer formation is an indicator of incompatibility in cell-cell adhesion in grafting (*12*–*14*). Thus, *Nb*/*Cm* grafts showed interfamily cell-cell adhesion. Unsuccessful interfamily *Gm*/*Cm* grafts had folded cell wall remnants caused by graft injury (Fig. 1G), whereas successful *Nb*/*At* interfamily grafts formed a thin cell wall at the graft interface (Fig. 1, H to K, and fig. S2). Thus, *Nb* can accomplish cell-cell adhesion in interfamily combinations.

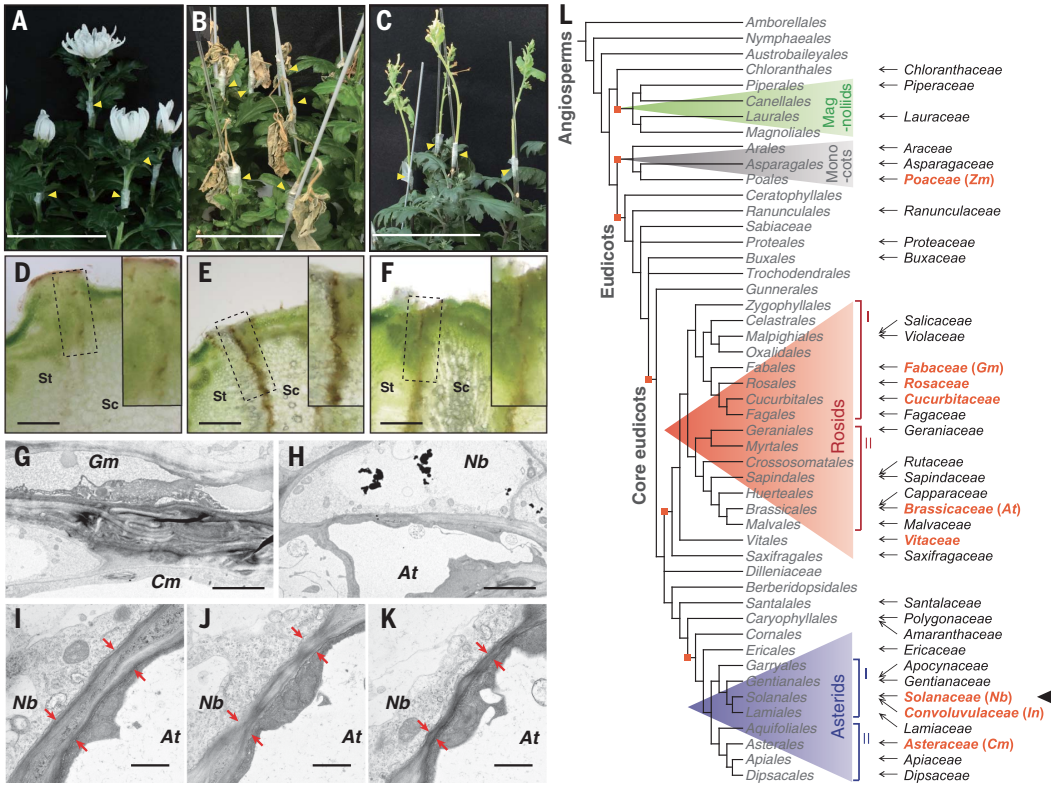

Fig. 1. *Nicotiana* interfamily grafting establishes through cell-cell adhesion. (**A** to **C**) Interfamily grafts, shown at 4 weeks after grafting between the *Cm*, *Gm*, and *Nb* scions, respectively, and the *Cm* stock. Yellow arrowheads denote graft junctions. Scale bars, 10 cm. (**D** to **F**) Transverse sections made at graft junctions shown in (A) to (C). Dashed rectangles indicate the position of insets. St, stocks; Sc, scions. Scale bars, 1 mm. (**G** and **H**) Transmission electron microscopy (TEM) images near the junction of the *Gm*/*Cm* (G) and *Nb*/*At* (H) interfamily grafts. Scale bars, 5 μm. (**I** to **K**) TEM images of serial sections of a cell-cell boundary at the graft interface of a *Nb*/*At* interfamily graft at 14 DAG. Arrows highlight the thickness of the cell wall between two cells. Scale bars, 1 μm. (**L**) Phylogenetic trees showing plant families for which *Nicotiana* plants (arrowhead) have preserved grafting beyond the family (arrows). Plant families including major crops are indicated in red. Abbreviations for plants used in transcriptome analysis are indicated in parentheses.

We then examined the range of angiosperms with which *Nicotiana* can establish grafts. We conducted grafting experiments using plants of seven *Nicotiana* species and an interfamily partner from 84 species in 42 families, chosen from among 416 angiosperm families (*16*). *Nicotiana* species, used as either scion or stock, supported interfamily grafting with 73 species from 38 families, including two species of magnoliids, five species of monocots, and 65 species of eudicots, including various vegetable, flower, and fruit tree crops (Fig. 1L, fig. S3, and tables S1 and S2). Thus, *Nicotiana* plants can graft to a range of angiosperms.

To examine the cellular mechanism of *Nicotiana* interfamily grafting, we analyzed transcriptomes at graft junctions from *Nb*/*At* interfamily grafts from 2 hours to 28 days after grafting (DAG) (Fig. 2). The transcriptome changed within 2 hours after grafting, and the state shifted further over time after grafting (Fig. 2, A and B). Genes associated with grafting (*17*, *18*) (table S3) whose expression was up-regulated in response to *Nb*/*At* interfamily grafting included genes associated with auxin action, wound repair, and cambium and vascular development (Fig. 2B). Their expression was comparable to, or higher than, that observed in *Nb*/*Nb* homografts (Fig. 2C). Transcriptomic changes at the graft junction were consistent with morphological changes in the *Nicotiana* interfamily grafts: Proliferation and xylem bridge formation were observed in the grafted region, but the xylem bundle was thin (fig. S4, A to E). Dye tracer experiments using toluidine blue, an apoplastic tracer, and carboxyfluorescein, a symplasmic tracer, showed establishment of both apoplastic and symplasmic transport at 3 DAG or later (fig. S4, F to H). Transport of mRNAs (*15*) and green fluorescent proteins across the heterograft junction was also detected (fig. S4, I and J) but was less than that for homografts. Hence, the viability of the *Nb* scions was preserved by parenchymatous tissue formation at the graft interface.

To elucidate the molecular events of graft formation, we identified 189 genes as early–up-regulated in the *Nb* scion of *Nb*/*At* interfamily grafts (Fig. 2D and table S3). Top Gene Ontology (GO) terms for these genes were

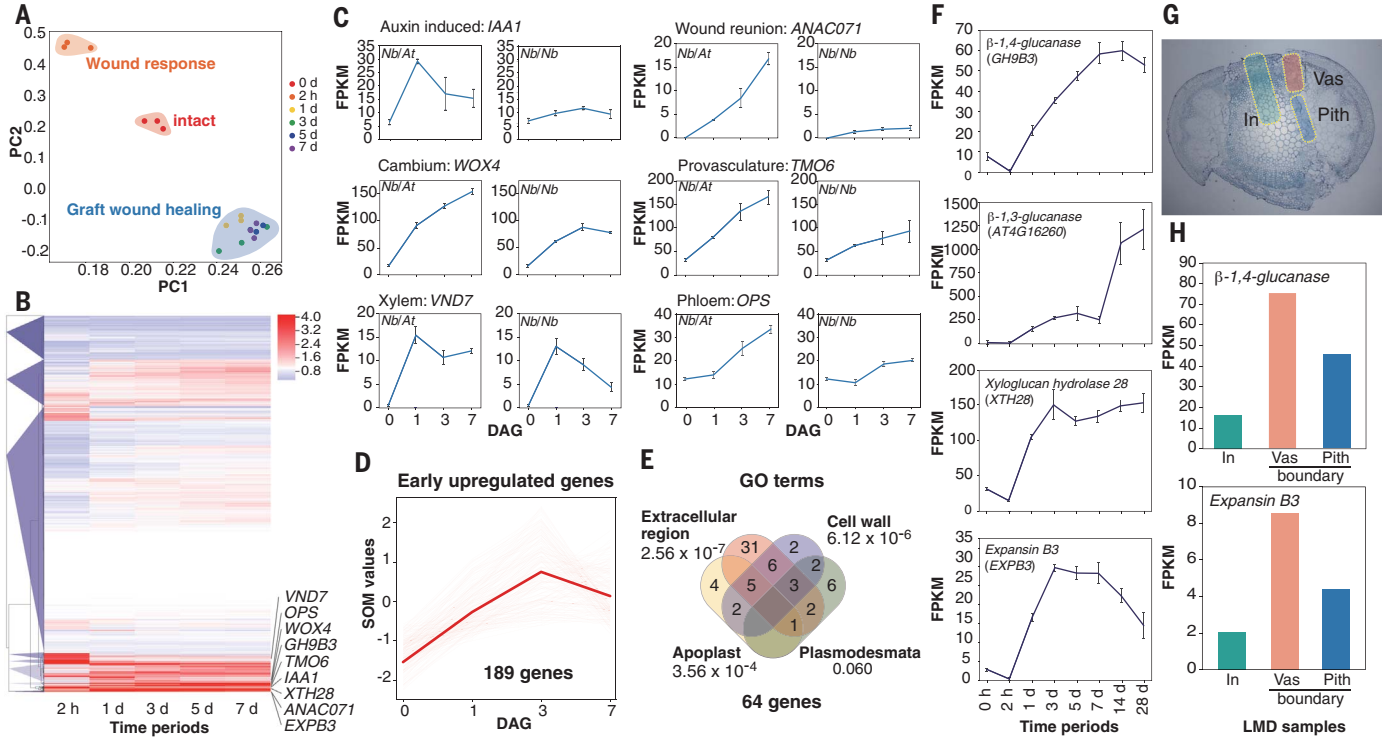

Fig. 2. Transcriptomic analysis reveals conventional graft-associated gene expression in *Nicotiana* interfamily grafting. (**A**) Principal components analysis of the transcriptome of the *Nb* intact stem and the scion of the *Nb*/*At* interfamily grafts at five time points (three biological replicates per time point). PC, principal component. (**B**) Hierarchical clustering with Euclidean distance and Ward's minimum variance method over ratio of RNA sequencing (RNA-seq) data from five time points after *Nb*/*At* grafting against intact plants. Genes for which association to grafting has been reported in previous studies are named. (**C**) Expression of genes associated with auxin action, wound reunion, and cambium, provasculature, xylem, and phloem development in *Nb*/*At* and *Nb*/*Nb* grafts. Table S3 provides details. FPKM, fragments per kilobase of transcript per million fragments mapped. (**D**) Extraction of early up-regulated genes for heterograft formation. See supplementary materials for extraction criteria. Profiles of 189 candidate genes are plotted against self-organizing map (SOM) values. Bold red line indicates the average of 189 genes. (**E**) GO enrichment analysis of 189 genes. Each numerical value represents the *P* value of GO analysis. (**F**) Expression profiles of representative genes after grafting. (**G**) Laser microdissection of *Nb*/*At* heterograft tissue was performed for the RNA-seq analysis. In, middle inside area of *Nb* scion tissue; Vas, cambial area of the graft boundary; Pith, pith area of the graft boundary. (**H**) Laser microdissection (LMD) RNA-seq of two of the genes shown in (F). Error bars in (C) and (F) denote SD.

[1]Bioscience and Biotechnology Center, Nagoya University, Furo-cho, Chikusa-ku, Nagoya 464-8601, Japan. [2]Graduate School of Bioagricultural Sciences, Nagoya University, Furo-cho, Chikusa-ku, Nagoya 464-8601, Japan. [3]Institute of Transformative Bio-Molecules, Nagoya University, Furo-cho, Chikusa-ku, Nagoya 464-8601, Japan. [4]GRA&GREEN Inc., Incubation Facility, Nagoya University, Furo-cho, Chikusa-ku, Nagoya 464-8601, Japan. [5]Graduate School of Science, Nagoya University, Furo-cho, Chikusa-ku, Nagoya 464-8601, Japan. [6]Department of Biosciences, Teikyo University, Utsunomiya, Tochigi 320-8551, Japan. [7]Center for Sustainable Resource Science, RIKEN, Tsurumi, Yokohama, Kanagawa 230-0045, Japan. [8]RIKEN BioResource Research Center, Tsukuba, Ibaraki 305-0074, Japan. [9]Graduate School of Science, University of Tokyo, Yayoi, Bunkyo-ku, Tokyo 113-8657, Japan. [10]College of Bioscience and Biotechnology, Chubu University, Matsumoto-cho, Kasugai 487-8501, Japan.
***Corresponding author. Email: notaguchi.michitaka@b.mbox.nagoya-u.ac.jp**

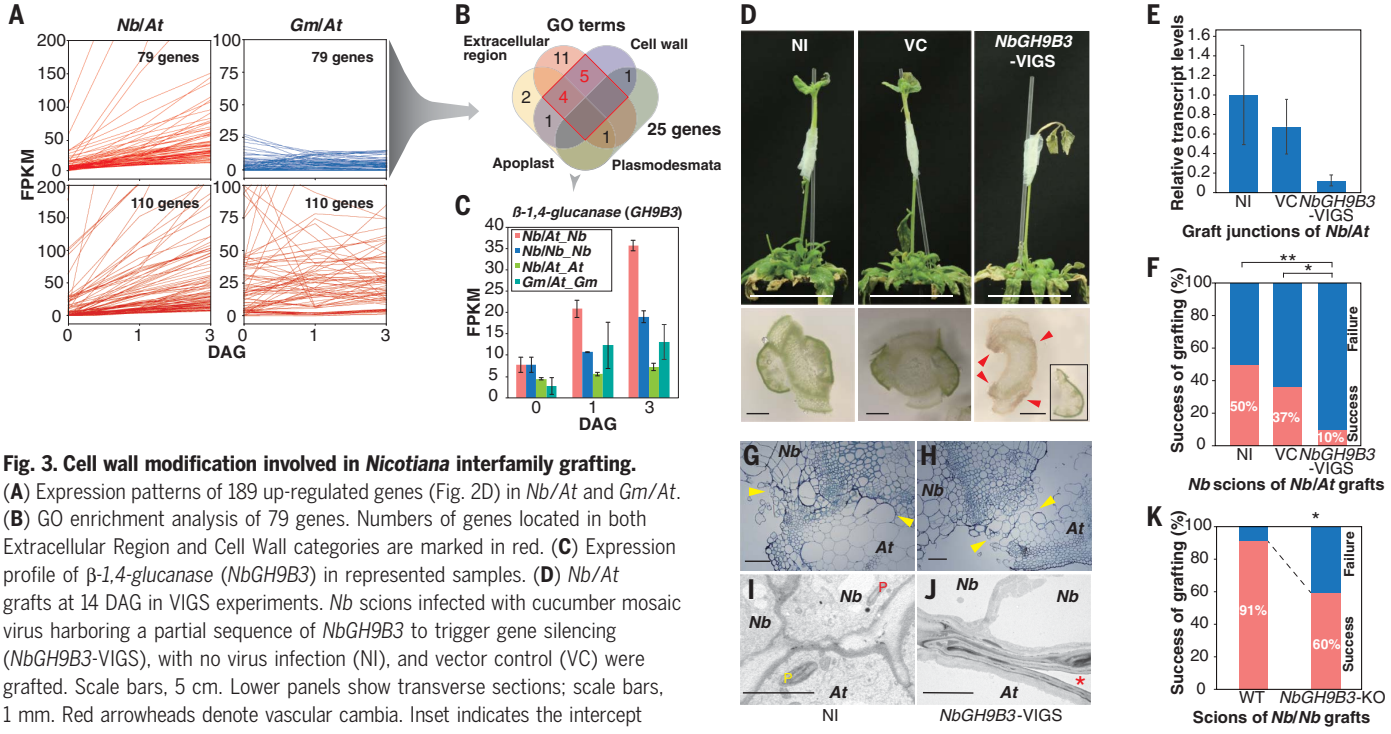

Fig. 3. Cell wall modification involved in *Nicotiana* interfamily grafting. (**A**) Expression patterns of 189 up-regulated genes (Fig. 2D) in *Nb/At* and *Gm/At*. (**B**) GO enrichment analysis of 79 genes. Numbers of genes located in both Extracellular Region and Cell Wall categories are marked in red. (**C**) Expression profile of β-*1,4-glucanase* (*NbGH9B3*) in represented samples. (**D**) *Nb/At* grafts at 14 DAG in VIGS experiments. *Nb* scions infected with cucumber mosaic virus harboring a partial sequence of *NbGH9B3* to trigger gene silencing (*NbGH9B3*-VIGS), with no virus infection (NI), and vector control (VC) were grafted. Scale bars, 5 cm. Lower panels show transverse sections; scale bars, 1 mm. Red arrowheads denote vascular cambia. Inset indicates the intercept of *At* tissues separated. (**E**) Suppression of *NbGH9B3* expression by VIGS was verified by quantitative reverse transcription polymerase chain reaction. (**F**) Effect of the *NbGH9B3*-VIGS on graft establishment. Differences between the sample groups were tested with Fisher exact tests with α set at $*P < 0.05$ or $**P < 0.01$, $n = 30$. (**G** to **J**) Transverse sections of grafted stem sample. [(G) and (H)] Optical microscope images. Yellow arrowheads indicate the boundary of *Nb* and *At*. Scale bars, 100 μm. [(I) and (J)] TEM images. Yellow P and red P indicate the plastids of *At* and *Nb*, respectively. Asterisk indicates a gap formed between *Nb* and *At* cells. Scale bars, 5 μm. (**K**) Effect of CRISPR knockout (KO) of *NbGH9B3* on graft establishment. Means were compared by Fisher exact test ($*P < 0.05$), $n = 45$ to 47. Error bars in (C) and (E) denote SD.

Extracellular Region, Cell Wall, and Apoplast (Fig. 2E and supplementary materials), implicating cell wall modification in *Nicotiana* interfamily grafting. Genes encoding cell wall modification/reconstruction enzymes, including β-1,4-glucanase, β-1,3-glucanase, xyloglucan hydrolase, and expansin, were up-regulated at 1 to 28 DAG (Fig. 2F). Laser microdissection samples of *Nb/At* interfamily graft junctions confirmed enhanced expression of a number of these genes in the cells that proliferated from the cambial or pith region of the graft boundary (Fig. 2, G and H). Transcriptomic studies of intrafamily grafting (*19*–*21*) and wounding response (*22*) also showed expression changes for genes associated with cell wall dynamics. Thus, *Nicotiana* activates cell wall reconstruction in both intrafamily and interfamily grafting.

By comparing interfamily grafting transcriptomes, we identified genes that were up-regulated in *Nb* scions of *Nb/At* interfamily grafts but not in soybean (*Gm*) scions of *Gm/At* interfamily grafts. We selected genes from *Gm* that showed the highest homology to each of the up-regulated *Nb* genes. Of 189 genes up-regulated in *Nb* scions (Fig. 2D), only 110 homologous genes in *Gm* scions were up-regulated (Fig. 3A and supplementary materials). We further analyzed the 79 homologous genes up-regulated in *Nb* but not *Gm* scions. Genes associated with Extracellular Region and Cell Wall were overrepresented in the 79 genes (Fig. 3B) (in comparison with Fig. 2E, the number of genes associated with Extracellular Region and Cell Wall was 9 out of 14, whereas the number of genes associated with the other GO terms was 16 out of 50). This result suggested that successful *Nicotiana* interfamily grafting requires cell wall reconstruction.

One gene expressed at *Nb* interfamily grafts was *NbGH9B3* (named on the basis of similarity to *At* genes), which encodes β-1,4-glucanase of the glycosyl hydrolase 9B (GH9B) family. The expression of *NbGH9B3* was up-regulated at 1 DAG and increased further at 3 DAG, but not significantly for that of the *Gm* homolog in *Gm/At* interfamily grafts (Fig. 3C). β-1,4-glucanases of the GH9B family function in cellulose digestion and cell wall relaxation or construction during plant growth processes such as root elongation (*23*, *24*). We hypothesized that *NbGH9B3* facilitates adhesion of facing cells at the graft boundary and further analyzed *NbGH9B3* function in grafting.

We applied virus-induced gene silencing (VIGS) to examine the function of *NbGH9B3* in *Nb/At* interfamily grafting (Fig. 3, D to F). Silencing of *NbGH9B3* caused failure of *Nb/At* interfamily grafting 2 weeks after grafting: The *Nb* scion was easily detached from the *At* stocks, and *Nb* tissues formed a necrotic layer on the graft surface (Fig. 3D). The amount of *NbGH9B3* expression reflected the success of grafting (Fig. 3, E and F). Folded cell walls, characteristic of failed grafts, were frequently observed at the graft interface of *Nb* scions in which *NbGH9B3* was down-regulated by VIGS, but not in noninfected controls (Fig. 3, G to J). We generated a knockout line of *NbGH9B3* (*NbGH9B3*-KO) using CRISPR/Cas9 editing (see supplementary materials). The percentage success of interfamily grafting onto *At* stocks was 91% for wild-type *Nb* scions and 60% for *NbGH9B3*-KO scions (Fig. 3K). Thus the β-1, 4-glucanase encoded by *NbGH9B3* facilitates graft establishment in *Nicotiana* interfamily grafting.

We next examined whether β-1,4-glucanase also functions in intrafamily grafting for other genera (Fig. 4, A and B), including soybean (*Gm*), morning glory (*In*), maize (*Zm*), and *Arabidopsis* (*At*). At *Gm*, *In*, and *At* homografts, one *GH9* family gene was up-regulated within 7 DAG; all belonged to the *GH9B3* clade (Fig. 4, A and B, and Fig. S5). For *Gm* and *In* scions grafted onto *At* stocks (Fig. 4B), *GH9B3* gene expression increased by 1 DAG and remained unchanged afterward. Thus, up-regulation of *GH9B3* gene expression during graft adhesion was conserved among these plants. *Zm*

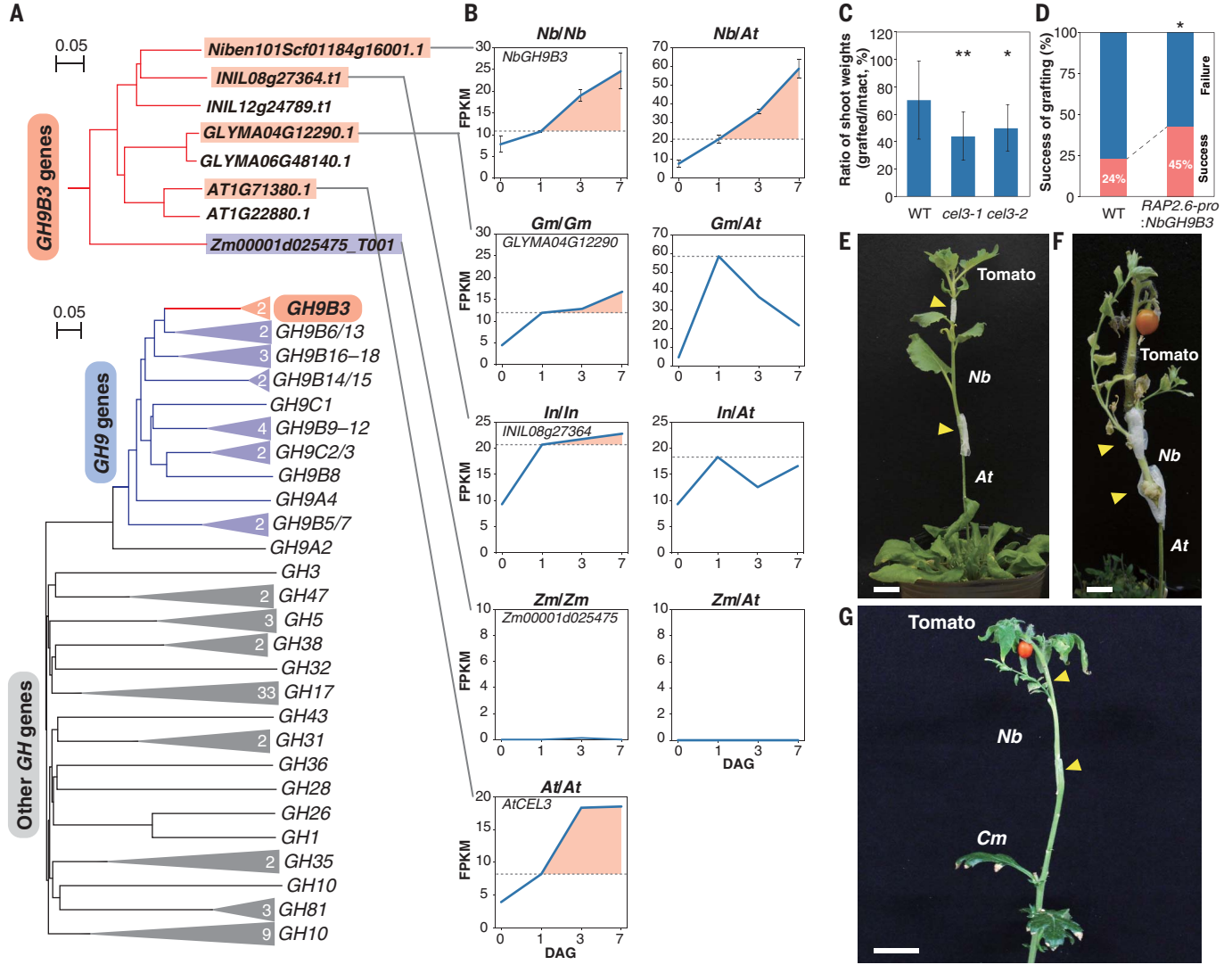

Fig. 4. Glycosyl hydrolase 9B3 is essential for graft wound healing in plants. (**A**) Phylogeny of plant glycosyl hydrolase gene family including the *GH9B3* clade. Top: Tree for the *GH9B3* clade genes. Bottom: Tree for all *GH* clades. Numbers of *At* genes included in each clade are shown in triangles (see supplementary materials). (**B**) *GH9B3* clade genes located in the same clade as *Niben101Scf01184 g16001* show a common expression pattern. (**C**) Increase in shoot fresh weight after grafting in two lines of mutants for *AtCEL3*. *P < 0.05, **P < 0.01 (Student t test); n = 14 to 19. (**D**) An *At* overexpression line of *NbGH9B3* using a RAP2.6 wound-inducible promoter (*NbGH9B3*-OX) increased percentage success of grafting relative to wild-type grafting (n = 64 and 102). Viability of the scion was determined at 14 DAG; the effect of overexpression was evaluated by Fisher exact test (*P < 0.05). (**E** to **G**) Grafts of tomato scion onto *At* [at 21 DAG (E) and 4 months after grafting (F)] or *Cm* [3 months after grafting (G)] using a *Nb* interscion. Yellow arrowheads indicate grafting points. Scale bars, 1 cm [(E) and (F)], 5 cm (G). Error bars in (B) and (C) denote SD.

homografts failed, as monocot species lack cambial activity in the stem (*25*). In *Zm* grafts, an orthologous gene was not up-regulated in either homografts or interfamily grafts.

To study *GH9B3* genes in grafting in other plant genera, we performed seedling micrografting in *Arabidopsis* using wild-type and two T-DNA insertion mutant lines for *CELLULASE3* (*AtCEL3*), a *GH9B3* clade gene that was up-regulated in *At* homografts (Fig. 4C). No significant difference in percentage success was observed between wild-type and *cel3-1* or *cel3-2* mutant homografts. However, shoot growth after grafting was decreased in grafts of both mutant lines relative to that of the wild type (Fig. 4C). Thus, GH9B3 is not required for establishment of the graft connection in *At* but does contribute to shoot growth after grafting (Fig. 3, F and K). To examine the effect of GH9B3 overexpression on grafting, we generated transgenic lines of *Arabidopsis* that overexpressed *NbGH9B3* under the control of a wound-induced *RAP2.6* promoter (*NbGH9B3*-OX) (*26*). The percentage success of micrografting using the *NbGH9B3*-OX line was significantly higher than that of wild-type grafting (Fig. 4D). Thus, GH9B3 functions in graft formation in *Arabidopsis* as well as in *Nicotiana*.

Our results show that *Nicotiana* plants use a mechanism for interfamily grafting that is generally activated only for intrafamily grafting. To exploit this capability, we examined whether *Nicotiana* could act as an intermediate in the grafting of different plant families. We grafted a tomato scion onto *At* or *Cm* stocks using a *Nicotiana* interscion. The *Nicotiana* interscion formed an intrafamily graft with the tomato scion and an interfamily graft with the *Cm* or *At* stocks. The tomato scions were successfully stabilized and produced fruit 3 to 4 months after grafting (Fig. 4, E to G, and fig. S6A). We also achieved other interfamily grafts in which the scion, interscion, and stock all belonged to different plant families (table S4 and fig. S6B).

Successful grafting requires wound response, cell regeneration, cell proliferation, cell-cell adhesion, and cell differentiation (*6*–*9*). *Nicotiana* shows graft compatibility with diverse plant species through the function of a conserved clade of extracellular-localized β-1,4-glucanases, the GH9B3 family, which probably target cellulose in cell walls (*23*, *27*). How the GH9B3 enzymes promote cell-cell adhesion is a key question for future research. Enhanced plant grafting techniques may increase the variety of root systems available to aid crop production with minimal destruction of ecosystems.

REFERENCES AND NOTES

1. K. Mudge, J. Janick, S. Scofield, E. E. Goldschmidt, *Hortic. Rev.* **35**, 437–493 (2009).
2. H. T. Hartmann, D. E. Kester, *Plant Propagation: Principles and Practices* (Prentice-Hall, ed. 3, 1975), pp. 314–427.
3. P. K. Andrews, C. S. Marquez, *Hortic. Rev.* **15**, 183–231 (1993).
4. C. W. Melnyk, *Regeneration* **4**, 3–14 (2016).
5. J. M. Lee, M. Oda, *Hortic. Rev.* **28**, 61–124 (2003).
6. E. E. Goldschmidt, *Front. Plant Sci.* **5**, 727 (2014).
7. J. Wang, L. Jiang, R. Wu, *New Phytol.* **214**, 56–65 (2017).
8. H. Tsutsui, M. Notaguchi, *Plant Cell Physiol.* **58**, 1291–1301 (2017).
9. B. S. Gaut, A. J. Miller, D. K. Seymour, *Annu. Rev. Genet.* **53**, 195–215 (2019).
10. S. V. Simon, *Jb. Wiss. Bot.* **72**, 137–160 (1930).
11. L. G. Nickell, *Science* **108**, 389 (1948).
12. R. Moore, D. B. Walker, *Am. J. Bot.* **68**, 831–842 (1981).
13. R. Kollmann, C. Glockmann, *Protoplasma* **124**, 224–235 (1985).
14. M. A. Flaishman, K. Loginovsky, S. Golobowich, S. Lev-Yadun, *J. Plant Growth Regul.* **27**, 231–239 (2008).
15. M. Notaguchi, T. Higashiyama, T. Suzuki, *Plant Cell Physiol.* **56**, 311–321 (2015).
16. Angiosperm Phylogeny Group, *Bot. J. Linn. Soc.* **181**, 1–20 (2016).
17. K. Matsuoka *et al*., *Plant Cell Physiol.* **57**, 2620–2631 (2016).
18. C. W. Melnyk *et al*., *Proc. Natl. Acad. Sci. U.S.A.* **115**, E2447–E2456 (2018).
19. S. J. Cookson *et al*., *J. Exp. Bot.* **64**, 2997–3008 (2013).
20. Y. Ren *et al*., *Plant Physiol. Biochem.* **129**, 368–380 (2018).
21. L. Xie, C. Dong, Q. Shang, *BMC Plant Biol.* **19**, 373 (2019).
22. Y. H. Cheong *et al*., *Plant Physiol.* **129**, 661–677 (2002).
23. D. J. Cosgrove, *Nat. Rev. Mol. Cell Biol.* **6**, 850–861 (2005).
24. D. R. Lewis *et al*., *Plant Cell* **25**, 3329–3346 (2013).
25. D. Roodt, Z. Li, Y. Van de Peer, E. Mizrachi, *Genome Biol. Evol.* **11**, 1986–1996 (2019).
26. K. Matsuoka *et al*., *Plant Mol. Biol.* **96**, 531–542 (2018).
27. B. R. Urbanowicz *et al*., *Plant Physiol.* **144**, 1693–1696 (2007).

ACKNOWLEDGMENTS

We thank D. Kurihara, T. Araki, K. Shiratake, S. Otagaki, S. Ishiguro, and Japan Tobacco Inc. for plant materials; C. Masuta for the VIGS vectors; A. Iwase for the *RAP2.6* plasmid vector; T. Shinagawa, H. Fukada, A. Ishiwata, R. Masuda, Y. Hakamada, M. Hattori, M. Matsumoto, I. Yoshikawa, A. Yagi, A. Shibata, and A. Furuta for technical assistance; and T. Akagi, Y. Hattori, and K. Toyokura for discussions. **Funding:** Supported by grants from the Japan Society for the Promotion of Science Grants-in-Aid for Scientific Research (18KT0040, 18H03950, and 19H05361 to M.No.; JP16H06280 and 19H05364 to Y.Sat.; 15H05959 and 17H06172 to K.S.), the Canon Foundation (R17-0070), the Project of the NARO Bio-oriented Technology Research Advancement Institution (Research Program on Development of Innovative Technology 28001A and 28001AB) to M.No., and the Japan Science and Technology Agency (ERATO JPMJER1004 to T.H.; START15657559 and PRESTO15665754 to M.No.). **Author contributions:** M.No., K.-i.K., Y.Sat., and M.Ni. conceived of the research and designed experiments; M.No. and K.O. performed grafting experiments; M.No. and Y.Saw. analyzed tissue sections; M.No. collected microscopic data with Y.Sat.'s support; R.T. performed VIGS experiments; Y.K. performed micrografting experiments; M.A. collected LMD samples; K.-i.K., R.O., and Y.I. generated RNA-seq libraries; T.S. performed sequencing; K.-i.K. analyzed transcriptome data; M.No., M.Ni., K.S., and T.H. supervised the experiments; and M.No., K.K., and M.Ni. wrote the paper. **Competing interests:** Nagoya University has filed for patents regarding the following topics: "Interfamily grafting technique using *Nicotiana*," inventor M.No. (patent publication nos. WO 2016/06018 and JP 2014-212889); "Grafting facilitation technique using cellulase," inventors M.No., K.K., R.T., and Y.K. (patent application nos. JP 2019-052727 and JP 2020-042379). T.H. is an adviser for GRA&GREEN Inc. **Data and materials availability:** RNA-seq data are available from the DNA Data Bank of Japan (www.ddbj.nig.ac.jp/) under accession number DRA009936. All other data are available in the main text or the supplementary materials. M.N. will handle requests for materials. All plasmid vectors and transgenic plants generated in this study are available from M.N. under a material agreement with Nagoya University.

SUPPLEMENTARY MATERIALS

science.sciencemag.org/content/369/6504/698/suppl/DC1
Materials and Methods
Figs. S1 to S6
Tables S1 to S5
References (*28*–*37*)
Movie S1
MDAR Reproducibility Checklist

View/request a protocol for this paper from *Bio-protocol*.

21 April 2020; accepted 12 June 2020
10.1126/science.abc3710